Direct ab Initio Dynamics Studies of the Reactions of H with $SiH_{4-n}Cl_n$ ($n = 1-3$)

Qingzhu Zhang, Shaokun Wang, and Yueshu Gu*

School of Chemistry and Chemical Engineering, Shandong University, Jinan 250100, P. R. China

Received: November 5, 2001; In Final Form: February 1, 2002

The direct hydrogen abstraction reactions of H atoms with SiH_3Cl, SiH_2Cl_2, and $SiHCl_3$ have been studied systematically using ab initio molecular orbital theory. Geometries have been optimized at the UMP2 level with the 6-311G(2d, p) basis set. The G3MP2 theory has been used for the final single-point energy calculation. Theoretical analysis provides conclusive evidence that the main process occurring in each case is the hydrogen abstraction from the Si−H bond; the chlorine abstraction from the Si−Cl bond has a higher barrier and is difficult to react. Changes of geometries, generalized normal-mode vibrational frequencies, and potential energies along the reaction path of the reactions are discussed and compared. The kinetic calculations of the title reactions have been deduced using canonical variational transition state theory (CVT) with the small-curvature tunneling (SCT) correction method over a wide temperature range of 200−3000 K. The CVT/SCT rate constants exhibit typical non-Arrhenius behavior. Three-parameter rate−temperature formulas have been fitted as follows: $k_1 = 1.54 \times 10^{-20}T^{3.03} \exp(-269.39/T)$, $k_2 = 1.93 \times 10^{-19}T^{2.62} \exp(-453.05/T)$, and $k_3 = 3.13 \times 10^{-19}T^{2.30} \exp(-249.99/T)$ for the reactions of H with SiH_3Cl, SiH_2Cl_2, and $SiHCl_3$, respectively (in units of cm^3 $molecule^{-1}$ s^{-1}). Studies show that chlorine substitution has no noticeable effect on the strength and on reactivity of the Si−H bond in $SiH_{4-n}Cl_n$ ($n = 1-3$). The calculated CVT/SCT rate constants are in excellent agreement with the available experimental values.

1. Introduction

Chlorosilanes are important materials in plasma chemical vapor deposition (CVD) processes and in semiconductor devices.[1−4] The reactions of chlorosilanes with atomic hydrogen, the simplest free-radical species, have drawn considerable attention: (1) Kinetic parameters for H-atom reactions are desirable not only to provide an uncomplicated probe of chemical reactivity but also to be helpful for a more extensive use of chlorosilanes. (2) A direct abstraction mechanism occurs in the reactions of atomic H with chlorosilanes:

$$SiH_3Cl + H \rightarrow SiH_2Cl + H_2 \quad (1)$$

$$SiH_2Cl_2 + H \rightarrow SiHCl_2 + H_2 \quad (2)$$

$$SiHCl_3 + H \rightarrow SiCl_3 + H_2 \quad (3)$$

(3) It has not been agreed whether chlorine substitution has an effect on the strength and on the reactivity trend of the Si−H bond. However, despite their practical and theoretical importance, the kinetics works about these reactions were very limited. Only one experimental study is on record: In 1989, Arthur[5] studied these reactions by a pulsed photolysis approach and obtained their rate-temperature formulas: $k_1(T) = (3.1 \pm 0.2) \times 10^{-11} \exp(-1418 \pm 23)/T$, $k_2(T) = (2.1 \pm 0.1) \times 10^{-11} \exp(-1459 \pm 19)/T$, and $k_3(T) = (0.27 \pm 0.02) \times 10^{-11} \exp(-1111 \pm 24)/T$ for the reactions of H with SiH_3Cl, SiH_2Cl_2, and $SiHCl_3$ (in cm^3 $molecule^{-1}$ s^{-1}). To our best knowledge, little theoretical attention has been paid to these reactions.

Here we present the first systematic theoretical study of the reactions of atomic H with chlorosilanes. Several important features of this work are the following: (1) The reaction mechanism has been revealed at high levels of ab initio molecule orbital theory. (2) The energy profile surface has been calculated at the G3MP2[6] theory level. (3) The rate constants have been obtained using canonical variational transition-state theory[7−9] with small curvature tunneling effect (CVT/SCT) correction over a wide temperature range of 200−3000 K. (4) The non-Arrhenius expression has been fitted. (5) The results of CVT/SCT calculations are compared with experimental values. (6) The effect of chlorine substitution on the strength and on the reactivity of the Si−H bond has been discussed.

2. Computation Methods and Theory

Ab initio calculations have been carried out using Gaussian 94 programs.[10] The geometries of reactants, transition states, and products have been optimized at the UMP2 level with the 6-311G(2d, p) basis set. The vibrational frequencies have been calculated at the same level to determine the nature of different stationary points and the zero-point energy (ZPE). The number of the imaginary frequency (0 or 1) confirms whether a bound minimum or a transition state has been located. The intrinsic reaction coordinate (IRC) calculation confirms that the transition state connects the designated reactants and products. At the UMP2/6-311G(2d, p) level, the minimum energy path (MEP) has been obtained with a gradient step size of 0.02 $amu^{1/2}$ bohr in a mass-weighted Cartesian coordinate for each reaction. The force constant matrixes of the stationary points and the selected nonstationary points near the transition state along the MEP have also been calculated for each reaction.

Although the geometrical parameters and the frequencies of various species can be determined satisfactorily at the UMP2/6-311G(2d, p) level, the energies obtained at this level may not accurate enough for the subsequent kinetic calculations. Therefore, a high and inexpensive theory level, G3MP2, was used for the energy calculation of the reactions of H with SiH_3Cl,

* Corresponding author. E-mail: guojz@icm.sdu.edu.cn.

10.1021/jp0140623 CCC: $22.00
Published on Web 03/20/2002

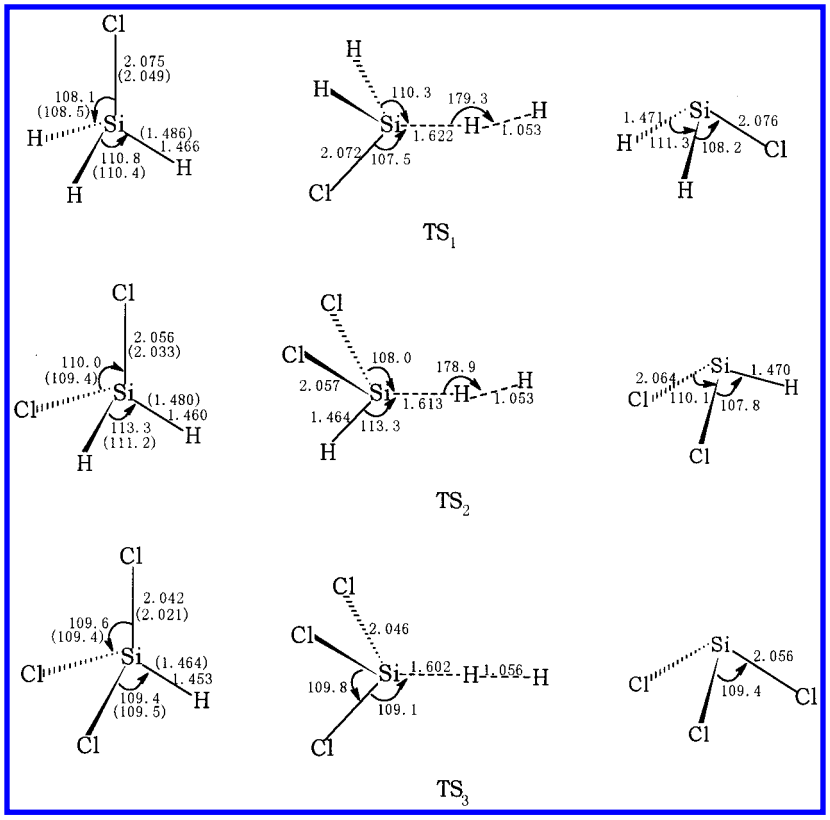

Figure 1. Optimized geometries for reactants, transition states, and products at the UMP2/6-311G(2d, p) level. The values in parentheses are the experimental data.[12] The bond length is in Å, and the bond angle is in deg.

SiH_2Cl_2, and $SiHCl_3$. The G3MP2 [6] energy is given as

$$E(\text{G3MP2}) = E[\text{QCISD(T)/6-31G(d)}] + E(\text{UMP2/G3MP2large}) - E[\text{UMP2/6-31G(d)}] + \text{HLC} + \text{ZPE}$$

where HLC is a high-level correction, HLC $= -0.004471n_\alpha - 0.004808n_\beta$, and n_α and n_β are the number of α and β valence electrons, respectively. It needs to be pointed that we have made two modifications in our G3MP2 calculations: (1) The geometries are obtained at the UMP2/6-311G(2d, p) level instead of MP2(FULL)/6-31G(d). (2) The zero point energies (ZPE) are obtained at the UMP2/6-311G(2d, p) level. All relative energies quoted and discussed in this paper include zero-point energy corrections with unscaled vibrational frequencies.

The initial information obtained from our ab initio calculations allowed us to calculate the variational rate constants including the tunneling effect. The canonical variational theory (CVT)[7-9] rate constant for temperature T is given:

$$k^{\text{CVT}}(T) = \min_s k^{\text{GT}}(T, s) \tag{4}$$

Here

$$k^{\text{GT}}(T, s) = \frac{\sigma k_B T}{h} \frac{Q^{\text{GT}}(T, s)}{\Phi^{\text{R}}(T)} e^{-V_{\text{MEP}}(s)/k_B T} \tag{5}$$

where $k^{\text{GT}}(T, s)$ is the generalized transition state theory rate constant at the dividing surface s, σ is the symmetry factor (the number of equivalent reaction paths, which was assumed to be 3, 2, and 1 for the reactions of H with SiH_3Cl, SiH_2Cl_2, and $SiHCl_3$, respectively), k_B is Boltzmann's constant, h is Planck's constant, $\Phi^{\text{R}}(T)$ is the reactant partition function/unit volume, excluding symmetry numbers for rotation, and $Q^{\text{GT}}(T, s)$ is the partition function of a generalized transition state at s with a local zero of energy at $V_{\text{MEP}}(s)$ and with all rotational symmetry numbers set to unity. The tunneling correction has been considered by using the centrifugal-dominant small curvature semiclassical adiabatic ground-state (CD-SCSAG) method. All the kinetical calculations have been carried out using the POLYRATE 7.8 program.[10] The MEP has been analyzed from $s = -2.0$ amu$^{1/2}$ bohr to $s = 2.0$ amu$^{1/2}$ bohr to converge the variational calculation. The step size of the Hessian calculation along the MEP was 0.02 amu$^{1/2}$ bohr.

3. Result and Discussion

The optimized geometries of reactants, transition states, and products are shown in Figure 1. The transition states of the reactions of H with SiH_3Cl, SiH_2Cl_2, and $SiHCl_3$ are denoted as TS_1, TS_2, and TS_3, respectively. The vibrational frequencies of reactants, transition states and products are listed in Table 1. Table 2 shows the Si−H bond dissociation energies calculated at various levels. Table 3 shows the potential barrier ΔE and the reaction enthalpy ΔH calculated for the reactions of H with chlorosilanes. The potential barrier ΔE and the reaction enthalpy ΔH calculated for the reaction of H with SiH_4 are also listed in Table 3 for comparison purposes. Figure 2 depicts the change curves of the classical potential energy (V_{MEP}) and vibrationally adiabatic potential energy curves (V_a^{G}) with the reaction coordinate s at the G3MP2//UMP2/6-311G(2d, p) level. Change curves of the generalized normal-mode vibrational frequencies with the reaction coordinate s are shown in Figure 3 for the reaction of H with SiH_3Cl. The calculated TST, CVT, and CVT/SCT rate constants along with the experimental values are presented in Figure 4.

3.1. Reaction Mechanism. It is worth stating the reliability of the calculations in this work. Since unrestricted Hartree−Fock (UHF) reference wave functions are not spin eigenfunc-

TABLE 1: Calculated Frequencies (in cm^{-1}) and the Zero-Point Energies (ZPE, in kcal/mol) for Reactants, Products, and Transition States Involved in the Reactions of H with $SiH_{4-n}Cl_n$ ($n = 1-3$) at the UMP2/6-311G(2d, p) Level[a]

species	frequencies	ZPE
SiH_3Cl	542, 682, 682, 981, 989, 989, 2350, 2362, 2362 *551, 663, 663, 945, 952, 952, 2201, 2211, 2211*	17.07
SiH_2Cl_2	189, 526, 586, 614, 737, 900, 984, 2378, 2394 *188, 527, 590, 602, 710, 876, 954, 2224, 2237*	13.31
$SiHCl_3$	176, 176, 254, 495, 602, 602, 825, 825, 2415 *176, 176, 254, 499, 600, 600, 811, 811, 2261*	9.11
SiH_2Cl	539, 671, 764, 950, 2300, 2332	10.80
$SiHCl_2$	181, 514, 574, 685, 775, 2306	7.20
$SiCl_3$	167, 167, 243, 476, 586, 586	3.18
TS1	1706i, 167, 293, 542, 679, 755, 961, 1025, 1035, 1151, 2330, 2350	16.14
TS2	1711i,170, 178, 191, 517, 586, 671, 780, 999, 1030, 1168, 2354	12.36
TS3	1709i, 163, 163, 183, 183, 244, 475, 599, 599, 979, 979, 1188	8.23

[a] The values in italics are the experimental data.[13]

TABLE 2: Si−H Bond Dissociation Energies at 0 K (BDE, in kcal/mol)[a]

BDE	UMP2/ 6-31G(d)	UQCISD(T)/ 6-31G(d)	G3MP2	expt
$D(SiH_3-H)$	73.73	75.60	90.08	90.4
$D(SiH_2Cl-H)$	77.37	78.89	90.32	
$D(SiHCl_2-H)$	77.78	79.09	90.48	
$D(SiCl_3-H)$	78.42	79.66	91.06	91.4

[a] The experimental values are obtained from ref 14.

TABLE 3: Potential Barriers ΔE (in kcal/mol) and Reaction Enthalpies ΔH (in kcal/mol) Calculated for the Hydrogen Abstraction Reactions of H with Silane and Chlorosilanes at the G3MP2//UMP2/6-311G(2d, p) Level[a]

reacns	ΔE	ΔH
$H + SiH_4$	3.11	−16.14
$H + SiH_3Cl$	3.05	−15.90
	18.57	*3.10*
$H + SiH_2Cl_2$	2.96	−15.73
	19.97	*5.75*
$H + SiHCl_3$	2.94	−15.15
	20.21	*6.57*

[a] The values in italics are the potential barriers and the enthalpies of the chlorine abstraction.

tions for open-shell species, we monitored the expectation values of $<S^2>$ in the UMP2 optimization. The values of $<S^2>$ are always in the range 0.750−0.776 for doublets at UMP2/6-311G-(2d, p) level. After spin annihilation, the values of $<S^2>$ are 0.750, where 0.750 is the exact value for a pure doublet. Thus, spin contamination is not severe in the UMP2/6-311G(2d, p) optimization for the title reactions. This suggests that a single determinant reference wave function for the title systems is suitable for the level of theory used in the optimization.[15]

To clarify the general reliability of the theoretical calculations, it is useful to compare the predicated chemical properties of the present particular systems of interest with experimental data. As shown in Figure 1, the calculated geometric parameters of SiH_3Cl, SiH_2Cl_2, and $SiHCl_3$ are in good agreement with the available experimental values. From this result, it might be inferred that the same accuracy could be expected for the calculated geometry parameters of the transition states. As can be seen from Table 1, the vibrational frequencies of SiH_3Cl, SiH_2Cl_2, and $SiHCl_3$ agree well with the experimentally observed fundamentals, and the maximum relative error is less than 7%. These good agreements give us confidence that the UMP2/6-311G(2d, p) theory level is adequate to optimize the geometries and to calculate the frequencies.

To choose a reliable theory level to calculate the energy, we calculated the dissociation energies of Si−H bonds in SiH_3Cl, SiH_2Cl_2, and $SiHCl_3$. The values at the UMP2/6-31G(d), UQCISD(T)/6-31G(d), and G3MP2 levels along with the experimental data are listed in Table 2. The dissociation energy of the Si−H bond in SiH_4 is also shown in Table 2 for comparison purpose. The experiments give the spectrum dissociation energy, and so the calculated dissociation energies have been corrected for the ZPE. The calculated results of $D(SiH_3-H)$ and $D(SiCl_3-H)$ at the G3MP2 level are in good agreement with the limited experimental values. Both the UMP2 and the UQCISD(T) level underestimate bond dissociation energies. So the G3MP2 theory is a good choice to calculate accurate energies for the title systems.

As mentioned above, the reactions of H with SiH_3Cl, SiH_2Cl_2, and $SiHCl_3$ can proceed via two channels: the hydrogen abstraction from the Si−H bond and the chlorine abstraction from the Si−Cl bond. As seen from Table 3, the barrier heights calculated at the G3MP2 level are 3.05, 2.96, and 2.94 kcal/mol for the hydrogen abstraction from SiH_3Cl, SiH_2Cl_2, and $SiHCl_3$, while the barrier heights of the chlorine abstraction are 18.57, 19.97, and 20.21 kcal/mol, respectively. The latter are much higher than the former. At the same time, the hydrogen abstraction is exothermic reaction, while the chlorine abstraction is endothermic reaction. Thus, we can safely say that the chlorine abstraction is negligible for these three reactions, which is very different from the mechanism of the reactions of H with CH_3Cl, CH_2Cl_2, and $CHCl_3$.[16] Therefore, we mainly discuss the hydrogen abstraction reactions from SiH_3Cl, SiH_2Cl_2, and $SiHCl_3$.

The transition states of the hydrogen abstraction from SiH_3Cl, SiH_2Cl_2, and $SiHCl_3$ are denoted as TS_1, TS_2, and TS_3, respectively. Their geometrical parameters calculated at the UMP2/6-311G(2d, p) level are shown in Figure 1. For the reactions of H with SiH_3Cl and SiH_2Cl_2, the H atom attacks one H of Si−H bonds with a slightly bent orientation angle of 179.3 and 178.9°, respectively. Thus, the transition states TS_1 and TS_2 have C_s symmetry. For the reaction of H with $SiHCl_3$, the H atom attacks linearly the H of the Si−H bond, and the transition state TS_3 has C_{3v} symmetry. For the transition states TS_1, TS_2, and TS_3, the breaking Si−H bonds are elongated by 10.64%, 10.48%, and 10.25%, while the forming H−H bonds are longer than the equilibrium value of 0.738 Å in H_2 by 42.68%, 42.68%, and 43.09%, respectively. Therefore, TS_1, TS_2, and TS_3 are reactant-like, and the hydrogen abstraction reactions proceed via early transition states. This rather early character in these transition states is in accordance with the low reaction barrier and the high exothermicity of these reactions, in keeping with Hammond's postulate.

Table 1 shows that transition states of the hydrogen abstraction from SiH_3Cl, SiH_2Cl_2, and $SiHCl_3$ have one and only one imaginary frequency. The values of the imaginary frequencies are large, which implies that the quantum tunneling effect may be significant and may play an important role in the calculation of the rate constant.

It is worth discussing the effect of chlorine substitution on the geometrical parameters and on the reaction mechanism for the reactions of H with SiH_4, SiH_3Cl, SiH_2Cl_2, and $SiHCl_3$. There are four features for the four reactions. First, the Si−H bond length in SiH_4 is 1.471 Å at the UMP2/6-311G(2d, p) level, while the Si−H bond lengths are 1.466, 1.460, and 1.453

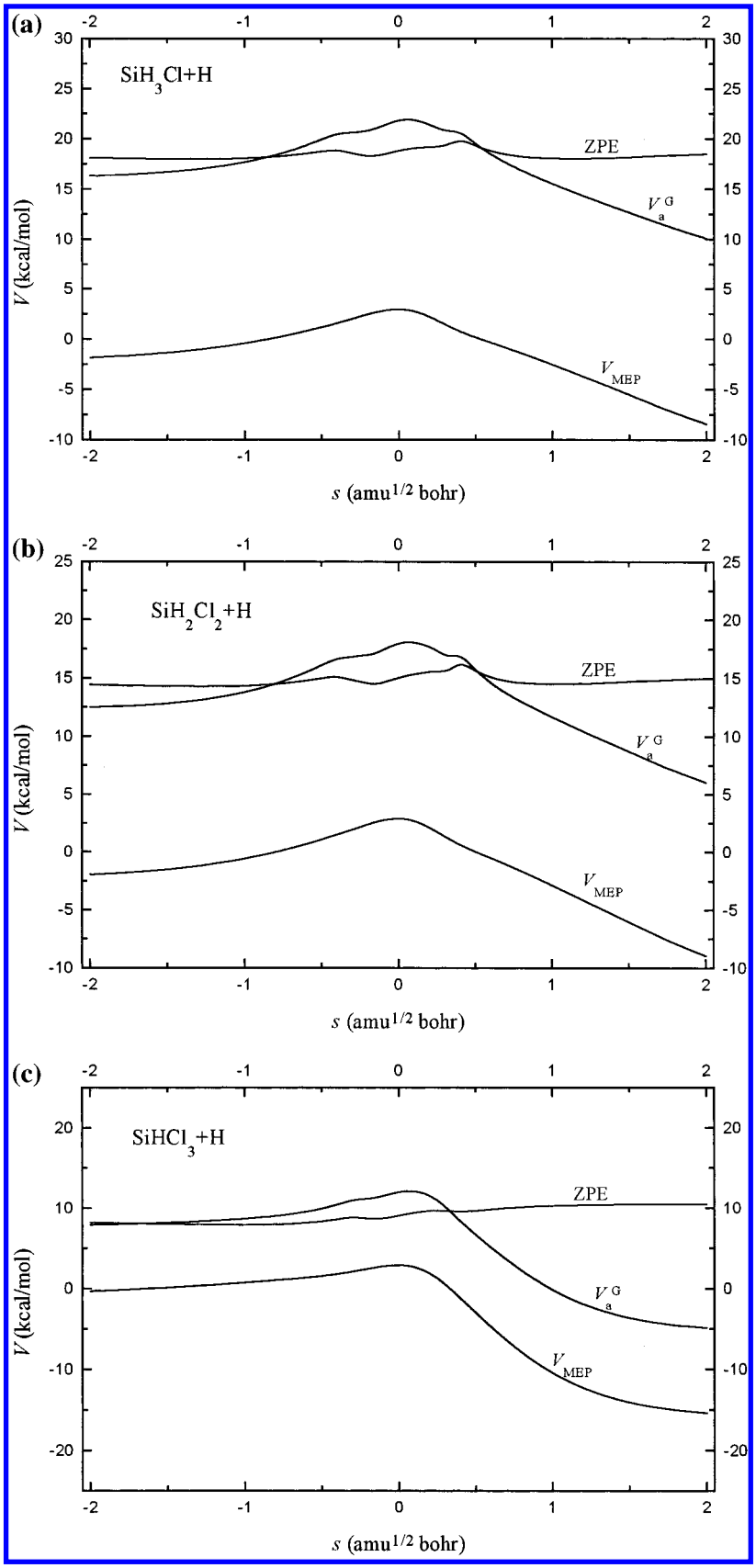

Figure 2. Classical potential energy (V_{MEP}) and the vibrationally adiabatic potential energy curves (V_a^G) as functions of s for the reactions of H with $SiH_{4-n}Cl_n$ ($n = 1-3$) at the G3MP2//UMP2/6-311G(2d, p) level.

Å in SiH_3Cl, SiH_2Cl_2, and $SiHCl_3$. There is a slight decrease in Si−H bond length along the series from SiH_4 to $SiHCl_3$. Second, the potential barrier of the reaction of H with SiH_4 is 3.11 kcal/mol at the G3MP2 level, while the potential barriers of the reactions of H with SiH_3Cl, SiH_2Cl_2, and $SiHCl_3$ are 3.05, 2.96, and 2.94 kcal/mol, respectively. The potential barriers of the reactions of H with silane and chlorosilanes are almost identical. Third, the reaction enthalpy of the reaction of H with SiH_4 is

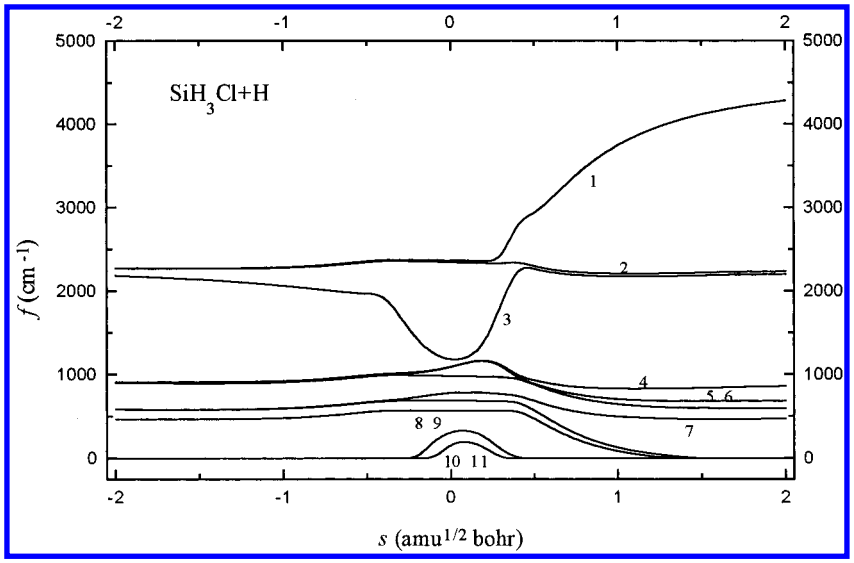

Figure 3. Changes of the generalized normal-mode vibrational frequencies as functions of *s* at the UMP2/6-311(2d, p) level for the reaction of H with SiH_3Cl.

−16.14 kcal/mol at the G3MP2 level, and the reaction enthalpies of the reactions of H with SiH_3Cl, SiH_2Cl_2, and $SiHCl_3$ are −15.90, −15.73, and −15.15 kcal/mol. The difference between the exothermicities for these four reactions is not large. Fourth, the dissociation energy of Si−H bonds in the SiH_4 is 90.08 kcal/mol at the G3MP2 level, while dissociation energies of Si−H bonds in the SiH_3Cl, SiH_2Cl_2, and $SiHCl_3$ are 90.32, 90.48, and 91.06 kcal/mol, respectively. The Si−H bond dissociation energies are almost identical in SiH_4, SiH_3Cl, SiH_2Cl_2, and $SiHCl_3$. It means that chlorine substitution has no noticeable effect on the reactivity and on the strength of the Si−H bond. The following study of the rate constants further testifies this view.

3.2. Kinetic Calculation. a. Reaction Path Properties. With a step size of 0.05 $amu^{1/2}$ bohr, the intrinsic reaction coordinate (IRC) has been calculated at the UMP2/6-311G(2d, p) level from the transition state to the reactants and the products for each reaction. For the reaction of H with SiH_3Cl, the breaking Si−H bond is almost unchanged from $s = -\infty$ to $s = -0.4$ $amu^{1/2}$ bohr, equals the value in the reactant, and stretches linearly after $s = -0.4$ $amu^{-1/2}$ bohr. The forming H−H bond shortens rapidly from reactants and reaches the equilibrium bond length in H_2 at $s = 0.5$ $amu^{1/2}$ bohr. Other bond lengths are almost unchanged during the reaction process. Therefore, the transition state TS_1 connects the reactants (SiH_3Cl and H) with the products (SiH_2-Cl and H_2). The geometric change mainly takes place in the region from $s = -0.4$ to $s = 0.5$ $amu^{1/2}$ bohr. The same conclusion can be drawn from the reactions of H with SiH_2Cl_2 and $SiHCl_3$.

The minimum energy path (MEP) is calculated at the UMP2/6-311G(2d, p) level by the IRC definition with a step size of 0.02 $amu^{1/2}$ bohr, and the energies of the MEP are further refined by the G3MP2//UMP2 method. For all the reactions the maximum position of the classical potential energy curve V_{MEP} at the G3MP2//UMP2/6-311G(2d, p) level corresponds to the saddle point structure at the UMP2/6-311G(2d, p) level. Therefore, the shifting of the maximum position for the V_{MEP} curve caused by the computational technique is avoided. The changes of the classical potential energy V_{MEP} and the ground-state vibrational adiabatic potential energy V_a^G with the reaction coordinate *s* are shown in Figure 2 for the reactions of H with SiH_3Cl, SiH_2Cl_2, and $SiHCl_3$. It is interesting to note that the change trend of V_{MEP} and V_a^G are similar for these three reactions, which means that they have a similar reaction mechanism. The maximum positions of V_a^G energy curves are 0.04, 0.09, and 0.13 $amu^{1/2}$ bohr at the G3MP2//UMP2 level for the reactions of H with SiH_3Cl, SiH_2Cl_2, and $SiHCl_3$, respectively, which implies that the variational effect may increase in going from SiH_3Cl to SiH_2Cl_2 to $SiHCl_3$. The zero-point energy ZPE, which is the difference of V_a^G and V_{MEP}, is almost unchanged as *s* varies. To analyze this behavior in greater detail, we show the variation of the generalized normal modes vibrational frequencies of the reaction of H with SiH_3Cl along the MEP in Figure 3.

Along the MEP a generalized normal-mode analysis has been performed using reactilinear Cartesian coordinate. In the negative limit of *s*, the frequencies are associated with the reactants, while, in the positive limit of *s*, the frequencies are associated with the products. For the sake of clarity, the vibrational frequencies can be divided into three types: spectator modes; transitional modes; reactive modes. The spectator modes are those that undergo little change and sometimes remain basically unchanged in going from reactants to the transition state. The transitional modes appear along the reaction path as a consequence of the transformation from free rotation or free translations within the reactant or the product limit into real vibrational motions in the global system. Their frequencies tend to zero at the reactant and the product limit and reach their maximum in the saddle point zone. The reactive modes are those that undergo the largest change in the saddle point zone, and, therefore, they must be related to the breaking/forming bonds. For the reaction of H with SiH_3Cl, mode 3 that connects the frequency of Si−H stretching vibration of SiH_3Cl with the frequency of the H−H stretching vibration of H_2 is the reactive mode, modes 10 and 11 are transitional modes, and other modes are spectator modes. From $s = -0.5$ to $s = 0.5$ $amu^{1/2}$ bohr, the reactive modes drop dramatically; this behavior is similar to that found in other hydrogen abstraction reactions.[17−19] A priori, this drop should cause a considerable fall in the zero-point energy near the transition state. But this kind of drop of the reactive mode is compensated partially by the transitional modes. As a result, the zero-point energy shows very little change with the change of the reaction coordinate *s*. The same conclusion can be drown form the reactions of H with SiH_2Cl_2 and $SiHCl_3$.

b. Rate Constants. Canonical variational transition state theory (CVT) with small curvature tunneling correction (SCT),

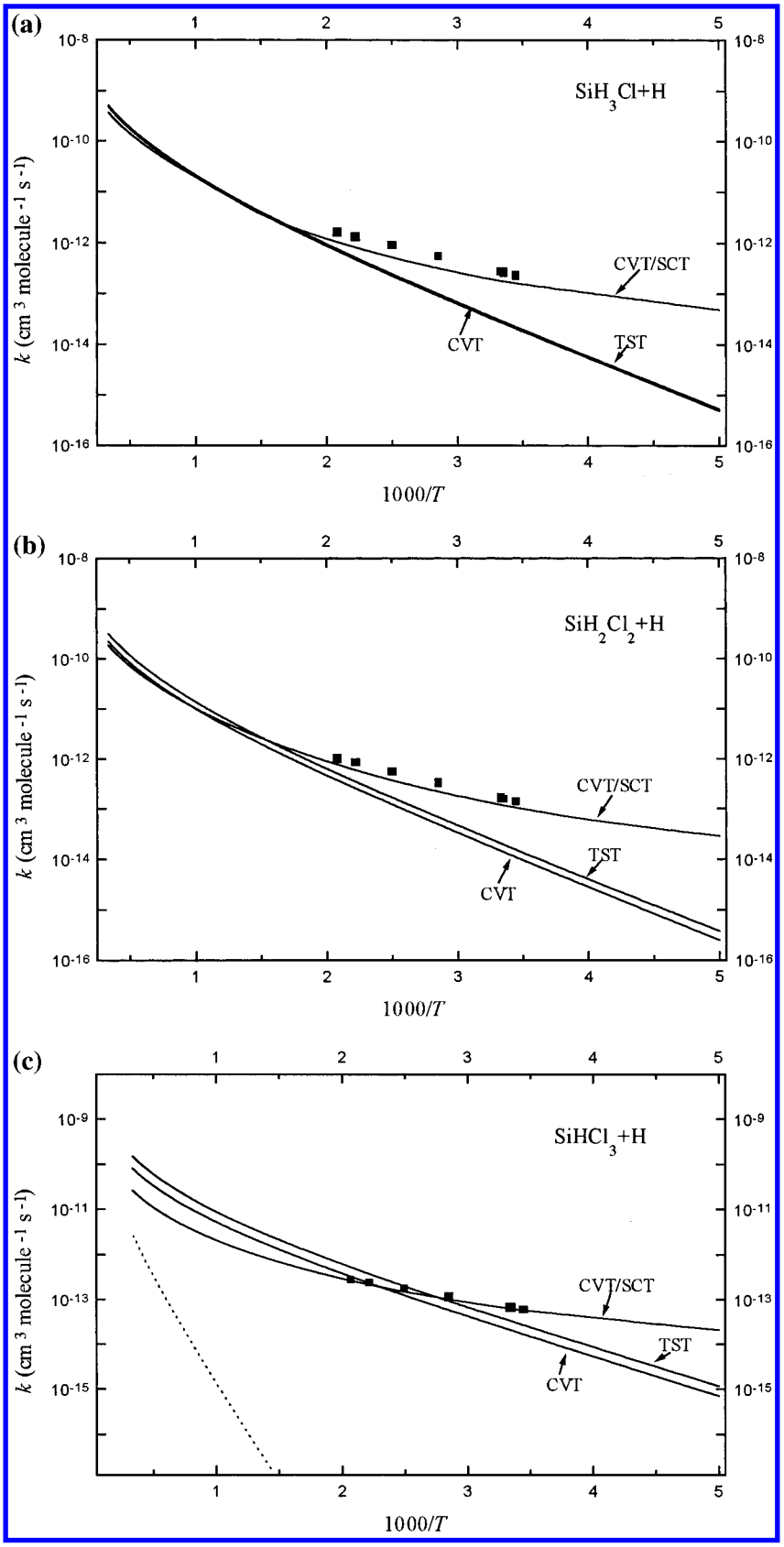

Figure 4. Rate constants as function of the reciprocal of the temperature (K) over the temperature range of 200−3000 K for the reactions of H with $SiH_{4-n}Cl_n$ ($n = 1-3$). ■ indicates the experimental values.[5]

which has been successfully performed for several analogous reactions,[20−21] is an effective method to calculate the rate constants. In this paper, we used this method to calculate the rate constants for the reactions of H with SiH_3Cl, SiH_2Cl_2, and $SiHCl_3$ over a wide temperature range from 200 to 3000 K.

To calculate the rate constants, 30 points are selected near the transition state along the MEP, 15 points in the reactant side and 15 points in the product side. The calculated CVT/SCT rate constants along with the experimental values are shown in Figure 4 for these three reactions. The calculated TST and

CVT are also depicted in Figure 4 for comparison purposes. Several features of the calculated rate constants are as follows:

(1) For each reaction the calculated CVT/SCT rate constants are in excellent agreement with the experimental values over the temperature range of 298−500 K. Therefore, the CVT/SCT method is a good choice to calculate accurate rate constants for the title systems.

(2) For the reaction of SiH_3Cl with H, the TST rate constants and the CVT rate constants are almost the same over the whole studied temperature range. For the reaction of SiH_2Cl_2 with H, the CVT rate constants are a little smaller than those of the TST. For the reaction of $SiHCl_3$ with H, the difference between the TST rate constants and the CVT constants is the biggest among these three reactions. It means there is an increase in variational effect in going from the reaction of SiH_3Cl with H to the reaction of $SiHCl_3$ with H. This conclusion is in good agreement with the above analysis.

(3) In the lower-temperature ranges, the CVT rate constants are much smaller than those of CVT/SCT, which means that the quantum tunneling effect is significant for these three reactions. In the higher temperature ranges, the CVT/SCT rate constants are close to those of TST and CVT for the reactions of H with SiH_3Cl and SiH_2Cl_2. This means only in the lower temperature ranges the small curvature tunneling correction plays an important role for these two reactions. For the reaction of H with $SiHCl_3$, in the temperature range of 1100−3000 K the CVT/SCT rate constants are smaller than the CVT values. For example, at 3000 K, the CVT rate constant is 8.06×10^{-11} cm^3 $molecule^{-1}$ s^{-1}, while the CVT/SCT rate constant is 2.69×10^{-11} cm^3 $molecule^{-1}$ s^{-1}. This shows that the transmission coefficients $\kappa_{SCT} < 1$, which means that the quantum tunneling effect is also significant for this reaction when the temperature is higher than 1100 K.

(4) It is obvious that the CVT/SCT rate constants exhibit typical non-Arrhenius behavior. The CVT/SCT rate constants of the title reactions are fitted by a three-parameter formula over the temperature range of 200−3000 K and given in units of cm^3 $molecule^{-1}$ s^{-1} as follows:

$$k_1 = 1.54 \times 10^{-20} T^{3.03} \exp(-269.39/T) \quad \text{H with } SiH_3Cl$$

$$k_2 = 1.93 \times 10^{-19} T^{2.62} \exp(-453.05/T) \quad \text{H with } SiH_2Cl_2$$

$$k_3 = 3.13 \times 10^{-19} T^{2.30} \exp(-249.99/T) \quad \text{H with } SiHCl_3$$

(5) The effect of chlorine substitution on the Si−H bond reactivity can be seen by evaluating the room-temperature *k/n*, the room-temperature rate constant corrected for the reaction-path degeneracy, where *n* is the number of Si−H bonds. At 298 K, *k/n* for the reaction of H with SiH_4[5] is 5.5×10^{-12} cm^3 $molecule^{-1}$ s^{-1}; for the reactions of H with SiH_3Cl, SiH_2Cl_2, and $SiHCl_3$, the values of *k/n* are 6.00×10^{-12}, 6.95×10^{-12}, and 6.40×10^{-12} cm^3 $molecule^{-1}$ s^{-1}, respectively. It can be seen that the effect of chlorine substitution on the room-temperature *k/n* value is small. The small effect of chlorine substitution on *k/n* is primarily due to the small change of potential barrier.

(6) To compare with the CVT/SCT rate constants of the hydrogen abstraction, the CVT/SCT rate constants of the chlorine abstraction from $SiHCl_3$ are also shown in Figure 4c (the imaginary line). It can be seen that the rate constants of the chlorine abstraction are much smaller than those of the hydrogen abstraction over the whole studied temperature range, and the contribution of the chlorine abstraction to the total rate constants can be negligible. For example, at 200 K, the CVT/SCT rate constant of the hydrogen abstraction is 1.6×10^{14} times larger than that of the chlorine abstraction, and at 3000 K, the CVT/SCT rate constant of the hydrogen abstraction is 10 times larger than that of the chlorine abstraction. If one takes into account the number of the Si−Cl bonds, the contribution of the chlorine abstraction to the total rate constants is much smaller for the reactions of H with SiH_3Cl and SiH_2Cl_2. Therefore, hydrogen abstraction is the sole channel for the reactions of H with SiH_3Cl, SiH_2Cl_2, and $SiHCl_3$, which is consistent with the above analysis.

4. Conclusion

In this paper, we have studied systematically the reactions of H with SiH_3Cl, SiH_2Cl_2, and $SiHCl_3$ using ab initio and canonical variational transition state theory (CVT) with small-curvature tunneling effect. Both the reaction mechanism and the rate constants were reported over the temperature range of 200−3000 K. Several major conclusions can be drawn from this calculation:

(1) Hydrogen abstraction from Si−H bonds is the sole channel for the reactions of H with $SiH_{4-n}Cl_n$ ($n = 1-3$).

(2) The three title reactions have similar reaction mechanism. The transition states involved in these reactions have rather early character.

(3) The calculated CVT/SCT rate constants exhibit typical non-Arrhenius behavior.

(4) Chlorine substitution has no noticeable effect on the reactivity and on the strength of Si−H bond.

Acknowledgment. The authors thank Professor Donald G. Truhlar for providing the POLYRATE 7.8 program. This work is supported by the Research Fund for the Doctoral Program of Higher Education of China.

References and Notes

(1) Beaucarne, G.; Poortmans, J.; Caymax, M.; Nijs, J.; Mertens, R. *Mater. Res. Soc. Symp. Proc.* **1998**, *485*, 89.

(2) Bisch, C.; Llauyo. G.; Wang, Y. B. *J. Appl. Phys*. **1998**, *3*, 47.

(3) Hiroyuki, N.; Kuniaki, Y.; Yukitaka, N. *Nippon Kessho Seicho Gakkaishi* **1998**, *25A*, 109.

(4) Kamimura, K.; Miwa, T.; Sugiyama, T.; Ogawa, T.; Nakao, M.; Onuma, Y. *Inst. Phys. Conf. Ser*. **1996**, *142*, 825.

(5) Arthur, N. L.; Potzinger, P.; Reimann B.; Steenbergen, H. P. *J. Chem. Soc., Faraday Trans. 2* **1989**, *85*, 1447.

(6) Curtiss, L. A.; Redfern, P. C.; Raghavachari, K.; Rassolov, V.; Pople, J. A. *J. Chem. Phys*. **1999**, *110*, 4703.

(7) Baldrige, K. K.; Gordor, M. S.; Steckler, R.; et al. *J. Phys. Chem*. **1989**, *93*, 5107.

(8) Gonzalez-Lafont, A.; Truong, T. N.; Truhlar, D. G. *J. Chem. Phys*. **1991**, *95* (12), 8875.

(9) Garrett, B. C.; Truhlar, D. G. *J. Phys. Chem.* **1979**, *83* (8), 1052.

(10) Frisch, M. J.; Trucks, G. W.; Schlegel, H. B.; Gill, P. W. M.; Johnson, B. G.; Robb, M. A.; Cheeseman, J. R.; Keith, T. A.; Petersson, G. A.; Montgomery, J. A.; Raghavachari, K.; Allaham, M. A.; Zakrzewski, V. G.; Ortiz, J. V.; Foresman, J. B.; Cioslowski, J.; Stefanov, B. B.; Nanayakkara, A.; Challacombe, M.; Peng, C. Y.; Ayala, P. Y.; Chen, W.; Wong, M. W.; Andres, J.; Replogle, E. S.; Gomperts, R.; Martin, R. L.; Fox, D. J.; Binkley, J. S.; Defrees, D. J.; Baker, J.; Stewart, J. P.; Head-Gordon, M.; Gonzales, C.; Pople, J. A. *GAUSSIAN94, Revision E.1*; Gaussian: Pittsburgh, PA, 1995.

(11) Steckler, R.; Chuang, Y. Y.; Fast, P. L.; Corchade, J. C.; Coitino, E. L.; Hu, W. P.; Liu, Y. P.; Lynch, G. C.; Nguyen, K.; Jackells, C. F.; Gu, M. Z.; Rossi, I.; Clayton, S.; Melissas, V.; Garrett, B. C.; Isaacson A. D.; Truhlar, D. G. *Polyrate 7.8 Version*; University of Minnesota: Minneapolis, MN, 1997.

(12) Cho, S. G.; Unwalla, R. J.; Cartledge, F. K.; Profeta, S., Jr. *J. Comput. Chem*. **1989**, *10*, 832.

(13) Su, M.-D.; Schlegel, H. B. *J. Phys. Chem*. **1993**, *97*, 8732.

(14) Wu, Y.-D.; Wong, C.-L. *J. Org. Chem*. **1995**, *60*, 821.

(15) Liu, R.; Francisco, J. S. *J. Phys. Chem. A* **1998**, *102*, 9869.

(16) Bryukov, M. G.; Slagle, I. R.; Knyazev, V. D. *J. Phys. Chem. A* **2001**, *105*, 3107.
(17) Espinosa-Garcia, J.; Corchado, J. C. *J. Phys. Chem.* **1996**, *100*, 16561.
(18) Corchado, J. C.; Espinosa-Garcia, J. *J. Chem. Phys.* **1997**, *106*, 4013.
(19) Espinosa-Garcia, J,; Corchado, J. C. *J. Phys. Chem.* **1997**, *101*, 7336.
(20) Yu, X.; Li, S. M.; Xu, Z. F.; Li, Z. S.; Sun, C. C. *Chem. Phys. Lett.* **2000**, *320*, 123.
(21) Yu, Y. X.; Li, S. M.; Xu, Z. F.; Li, Z. S.; Sun, C. C. *Chem. Phys. Lett*. **1999**, *302*, 281.